ANN-Based: WRIM Speed Control and Harmonic analysis of Rotor Chopper Resistance

Ismael K. Saeed
E-mail: ismailgardy@gmail.com
Department of Electrical Engineering
College of Engineering
University of Salahaddin
Iraq

Hilmi F. Ameen
E-mail:hfameen@gmail. com
Department of Electrical Engineering
College of Engineering
University of Salahaddin
Iraq

Abstract

This paper presents an Artificial Neural Network (ANN) based technique for controlling external chopper resistance circuit in the rotor side of wound rotor induction motor(WRIM), for keeping the motor speed constant at the varied torque or keeping the load torque constant at the varied speed , which generates the exact chopper duty cycle for any given operating condition.

Also the paper study current and torque harmonics analysis. The controller circuit was simulated and operated on both closed and open loops. Theoretical analysis is carried out for the controller drive system. Theoretically obtained results are compared with those obtained by ANN. All data which are used to train the network by a back propagation algorithm simulated in the MATLAB Neural Network Toolbox. The results obtained are satisfactory and promising. The advantages of this controller have the design simplicity and high accuracy.

Key Words: Wound Rotor Induction Motor (WRIM), Rotor Chopper Resistance Circuit, Artificial Neural Network(ANN).

الخلاصة

يعرض هذا البحث استخدام تقنية شبكة الخلايا العصبية الصناعية للسيطرة على محرك حثى من نوع الدوار الملفوف باستخدام تقنية تغيير مقاومة الدوار عن طريق المقطع لتثبيت السرعة عند تغيير العزم او تثبيت العزم عند تغيير السرعة والتى تودى الى ايجاد عرض النبضة الملائم و الحقيقى لايجاد نقطة التشغيل وايضا يتناول البحث دراسة و ايجاد التوافقيات للتيار والعزم وايجاده بواسطة تقنية شبكةالخلايا العصبية الصناعية .

و قد اخذت النتائج المحاكاة للدائرة المستخدمة للسيطرة فى حالة دارة المفتوحة و المغلقة وقد تم مقارنة النتائج التى حصلنا عليه نظريا مع التى حصلنا عليه بواسطة تقنية شبكةالخلايا العصبية الصناعية .وقد تم تعليم و تدريب شبكةالخلايا العصبية الصناعية بواسطة البرنامج MATLAB و قد كانت النتائج التى حصلنا عليها مرضية كما ان نظام السيطرة المعتمد بسيط و ذو دقة جيدة.

1.Introduction

Induction motors are the workhorses of industry because of their low cost and rugged construction. It is used in the process control industry to adjust speed for fans, compressors, pumps, and induction motor drives for electric traction. When operated directly from line voltages, induction motors operate at a nearly constant speed. However, by means of power electronic topologies, it is possible to vary their speed efficiently [1].

The static rotor chopper resistance control of WRIMs is the simplest and cheapest method, because it requires the minimum number of components in rotor side, one resistance, one power electronic devices. The disadvantages of this method is dissipative of power in external resistance makes it low efficiency.

The construction of three phase WRIM is particularly adapted to large torque and high power requirements. The rotor is wound with a three-phase winding which is interconnected to a rotor load circuit for absorbing the energy associated with the inherent slip characteristic of wound rotor motors. Resistance elements may be connected into the rotor load circuit to boost the starting torque of the motor and change the speed-torque characteristic. This results in a relatively inefficient operation but has been used in many installations, particularly with switching means to insert and remove resistance so as to adjust the motor characteristic, such as, cranes, hoists, elevators ...etc. It can preferable to use wound rotor motors with a changeable resistance rotor circuit. The efficiency of rotor resistance control method is low at reduced speed because of higher slips. However, in applications where low speed operation is only a small proportion of the work, the low efficiency is acceptable. Typical application of the rotor resistance control method is the hoist drives of a shop crane. This method also can be used in fan or pump drives, where variation speed over a small range near the synchronous speed is required. Different attempts have been made to use SCR's with different configuration in the rotor circuit to have continuous and contact less effective resistance impedance control. Controlling the effective rotor resistance by varying the chopper-duty cycle was discussed briefly in [2 – 6].

Chopper resistance control is used to improve the dc dynamic braking of WRIMs, the braking time and energy loss are considerably reduced in[7].The starting transient behaviors of chopper resistance control of WRIMs, by properly controlling duty cycle to adjust rotor resistance with high output torque and low starting current was obtained in [8]. Several starting techniques of three phase WRIMs was investigated and compared by using rotor resistance and double feed starting by [9]. Developing an alternative branch of the control theory based on the computation technologies of artificial neural networks make it possible to improve the existing algorithms and to develop new branches [10]. The ANN-based chopper controlled of wound rotor induction motor was used to operate in open loop and to achieve motor soft starting using thyristors as switches [11].

This paper presents an ANN-based chopper controlled WRIM in which the appropriate chopper duty cycle is found as a function of required motor speed and load torque. The power MOSFET is chosen as a chopper switch to provide complete system of both open and closed loops, because of its high switching frequency and simple drive circuit.

2. Performance Analysis of Rotor Chopper Drive

2.1 Torque and speed regulation of the drive

Theoretically, WRIMs can be operated with limited- current or higher starting torque by selecting an appropriate value of the rotor resistance. As the rotor speeds up, the external resistance is decreased accordingly to match the operating requirements. The chopper in Figure 1 is a power switching device changes the external resistance in a continuous, smooth and contact less manner. By regulating the duty cycle of the chopper, it is possible to obtain an equivalent resistance of a value between zero and the value of external resistance. The duty cycle(δ) of the chopper is defined as [4]:

$$\delta = \frac{T_{on}}{T_{ch}} \tag{1}$$

where T_{on} is the time interval of the "on" state, and T_{ch} is the chopping period of the chopper. The MATLAB program Neural Network Toolbox used for WRIM with rotor chopper circuit to simulate the drive circuit performance. The following assumptions are made for performance analysis of the rotor chopper drive: (1) No commutation overlap in the diode bridges. (2) There are ripple free dc currents. (3) The supply phase currents and the rotor phase currents will have six-step waveforms. (4) No losses in diode-bridge and power-switches [3]. According to Figure 1, the mathematical model of system is analyzed by considering a simplified equivalent circuit of dc link with chopper. Then the rotor rectified current (I_{dc}) can be determined from[13],

$$I_{dc} = \frac{3\sqrt{6}sE'_1}{\pi(2R_1' + \frac{3(X_1'+X_2)s}{\pi} + 2R_2 + R_f + R_{ex}(1-\delta)} \tag{2}$$

Where, s is the slip, ω_s is the angular supply frequency in rad/sec, E_1 rotor rms value per phase at standstill, R_1' and X_1' are stator resistance and leakage reactance referred to rotor side, R_2 and X_2 are rotor resistance and leakage reactance per phase, R_f is the smoothing resistance, and R_{ex} is the external rotor resistance in rotor side. Then the electromagnetic torque developed equation can be obtained from the dc circuit [12]:

$$T_e = \{[(3\sqrt{6}\,sE_1/\pi) - (3s(X_1' + X_2)I_{dc}/\pi)]I_{dc} - 2sR_1 I_{dc}^2\}/s\omega_s \tag{3}$$

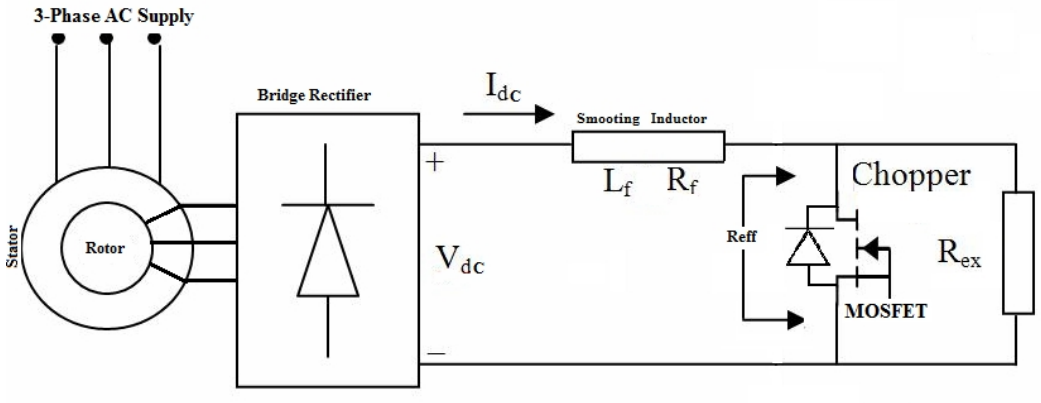

Figure 1. Chopper controlled induction motor

2.2 Harmonic Analysis

The full set of harmonics can be represented by a Fourier series to show the original wave form. If the waveform of the rotor phase current is assumed to be a square pulses of a six stepped wave shape, then the Fourier serious can be written as[13];

$$i_r = \frac{2\sqrt{3}}{\pi} I_{dc} \left\{ \begin{array}{l} \sin(s\omega_s t + \phi_1) - \frac{1}{5}\sin(5s\omega_s t + \phi_5) + \frac{1}{7}\sin(7s\omega_s t + \phi_7) - \\ \frac{1}{11}\sin(11s\omega_s t + \phi_{11}) + \frac{1}{13}\sin(13s\omega_s t + \phi_{13}) - \ldots\ldots\ldots . \end{array} \right\} \quad (4)$$

Where, s is the slip, i_r is the rotor phase current, I_{dc} is the rotor rectified current and ω_s are the angular supply frequency in rad/sec. According to Figure 1, the mathematical model of system is analyzed by considering a simplified equivalent circuit of dc link with chopper. With harmonic order determined from the expression (n=6k±1). The magnitude of the fundamental rotor current can be given by [13];

$$I_{rf} = \frac{\sqrt{6}}{\pi} I_{dc} \quad (5)$$

And the magnitude of the n[th] harmonic can be given by;

$$I_{rn} = \frac{\sqrt{6}}{n\pi} I_{dc} \quad (6)$$

The harmonic slip s_n , which is defined as the stator harmonic frequency to the rotor harmonic frequency[13,14]. In general it can be written;

$$s_n = \frac{1 \mp (n \pm 1)}{ns} \quad (7)$$

The harmonic slip s_n is contained the fundamental slip s, thus all reactance are increased by a factor n. Actually, the rotor harmonic current will be distributed in parallel between the stator and the magnetic circuits. The stator phase current therefore consists of a series of blocks or pulses per half cycle which represent a fundamental sine wave plus numerous harmonics. Therefore, the magnitude of the current in the stator by n[th] harmonic current is;

$$I_n = \frac{I_{rf}}{n} \left[\frac{jnsX'_m}{\frac{R'_1}{s_n} + jns(X'_1 + X'_m)} \right] \quad (8)$$

In a three phase bridge rectifier or inverter, all even harmonics of current and those divisible by three are absent on the ac side. hence only the 5[th], 7[th], 11[th], 13[th] etc are present. [15]. The harmonic forced in to the rotor by rectification process produce pulsating torque, which can be derived by the n[th] harmonic of rotor current injected to the stator so that the n[th] harmonic torque is;

$$T_n = \frac{I_n^2 * R_1}{n * s * s_n * \omega_s} \quad (9)$$

All torques have an odd order, with the 5[th], 11[th], 17[th], 23[rd] etc components aiding the fundamental and the 7[th], 13[th], 19[th], 25[th] etc components opposing the fundamental.
The net effect of all these steady aiding and opposing torque components is a slight reduction in the value of the net steady state torque of the motor [15].

3. Artificial Neural Networks

The application of artificial neural networks (ANNs) is recently growing in the power electronics and drives areas. ANNs have been proved to be capable of learning from raw data. They can be used to identify relations within raw data not explicitly given or even known by human experts and there is no need to assume any linear relationship between data [16].

Of all the ANNs, the multi-layer feed forward artificial neural network, trained using the back-propagation algorithm, is the most commonly and flexibly used [17]. Its typical architecture, which contains the input layer, a number of hidden layers and the output layer, is shown in Figure 2.

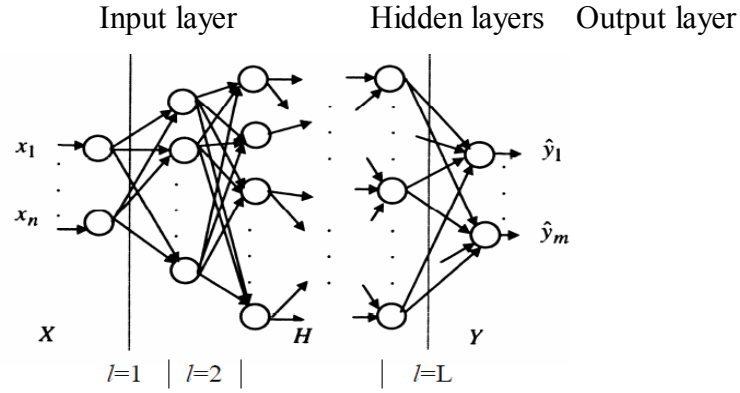

Figure 2. A multi-layer feed forward artificial neural network architecture

By the algorithmic approach known as Marquardt–Levenberg (ML) back propagation algorithm, the error is decreased repeatedly. Some ANN models employ supervisory training while others are referred to as none-supervisory or self organizing training. However, the vast majority of ANN models use supervisory training. The training phase may consume a lot of time. In the supervisory training, the actual output of ANN is compared with the desired output. The training set consists of presenting input and output data to the network. The network adjusts the weighting coefficients, which usually begin with random set, so that the next iteration will produce a closer match between the desired and the actual output. The training method tries to minimize the current errors for all processing elements. This global error reduction is created over time by continuously modifying the weighting coefficients until the ANN reaches the user defined performance level [18].

In order to use the ANN simulator for any application, first the number of neurons in the layers, type of activation function (purelin, tansig, logsig), the number of patterns, and the training rate must be chosen [18]. We define the input vector to the network $X=[x_1,x_2,\ldots,x_n]^T$ and output vector $Y=[y_1,y_2,\ldots,y_m]^T$ where n is the number of input layer and m is the number of output layer neurons. Each layer is represented by l, i.e., input layer (l=0), hidden layers (l=1,2,3…L-1), and output layer (l=L) and each neuron in the hidden and output layer receives signals $v=[v_1,v_2,\ldots,v_k]^T$ from the neurons of the previous layer, scaled by the weights $w_j=[w_{j1},w_{j2},\ldots,w_{jk}]^T$.

The activity level of the jth neuron in layer l is obtained as (4):

$$o_j = f_j(Net_j) = f_j[\sum_{i=1}^{k}(w_{ji}v_i) + b_i] \quad (10)$$

where o_j is the activity level (output) of the jth neuron, Net_j is the input of the jth neuron, f_j is the activation function of the jth neuron, w_{ji} is the connection weight from the ith neuron to the jth neuron, v_j is the activity level of the ith neuron in the prior layer and b_j is the bias term of the jth neuron. The active function defines the output of a neuron in terms of the activity level at its level. There are three basic types of activation functions: threshold, piece-linear and sigmoid [17]. The sigmoid function is by far the most common activation function. The tan-sigmoid transfer function is used, which generates outputs between -1 and +1. Its definition is expressed in equation (5):

$$f(Net_j) = \frac{1}{1+e^{-2Net_j}} - \frac{1}{1+e^{2Net_j}} \quad (11)$$

The back propagation algorithm is used to train the network [17]. The connection weights are iteratively adjusted so that the error between the network output and the desired output (target) for a given reference input is minimized. The error goal is expressed as the mean squared error (MSE), calculated as follows:

$$MSE = \frac{1}{m}\sum_{k=1}^{m}(t_k - y_k)^2 \quad (12)$$

where t_k represents the desired output of the kth neuron in the output layer.

Learning continues iteratively until the mean of the squared error is below a certain goal. In order to improve the neural network performance, the data must be well-processed and properly-scaled before inputting them to ANN. The normalization process was required to restrict the range of the patterns for input into the neural networks. Normalization of data is a process of scaling the numbers in a data set to improve the accuracy of the subsequent numeric computations and is an important stage for training of the ANN. Normalization also helps in shaping the activation function [17].

In this paper multi layer feed forward network with ML back propagation training algorithm is used. The typical multi-layer architecture used for the duty cycle calculation. The inputs to the neural network are normalized between (–1 , +1). It has a hidden layer of tansigmoidal with purelinmoidal , neurons which receives inputs (the motor speed and the load torque) directly, then broadcast their outputs to a layer of linear neurons, which compute the network output (the duty cycle).

4. Simulation Model

The network's architectures were decided empirically by using trial and error method for choosing best ANN structure which is involved to training and testing different number of networks. It is difficult to know how large a network should be for a specific application. If a larger network is used the more complex functions of the network can be created and if small enough networks are selected, they will not have enough power to over fit the data. Various networks with different number of neurons in their hidden layers were trained with ML algorithms [19].

The number of layers and the number of processing elements per layer are important decisions for selecting the ANN architecture. Choosing these parameters to a feed forward back propagation topology is the art of the ANN designer. The training process has been stopped when the system has been stable [18, 19].

To check the accuracy of the designed ANN model, the actual values of duty cycle obtained by simulation were compared with those values obtained by ANN. The newly generated sets of speed and torque patterns are input to the MATLAB neural net model and the corresponding values of duty cycle δ are calculated systematically. After normalization all data the ANN model was implemented by software and incorporated in the drive system program as shown in Figure 3.

Both the reference speed (n_{ref}) and load torque (T_L) are input to the ANN model, which produces the appropriate chopper duty cycle (δ). A firing circuit generates pulse to the power MOSFET is chosen as a chopper switch with the corresponding duty cycle. The neural network program was run in several cases; fixed chopper duty cycle and varying load torque and speed, fixed torque and varying speed, and a fixed speed and varying torque are taken. The system parameters used in the simulation are:

380/220V, 3.75/6.5A, Y/ Δ, 2.25 kW, 50Hz, 4-pole, WRIM, N_s/N_r=3.1667, R_s=4.125Ω, R_r = 0.359Ω, L_s = 20.5mH, L_r = 1.6mH, R_f= 0.05Ω, L_f= 10mH, X_m = 120.5741 Ω, $E_1^{/}$=69.473V, R_{ex} = 30Ω, f_{ch} = 5kHz, M = 250mH, J = 0.08kg.m^2.

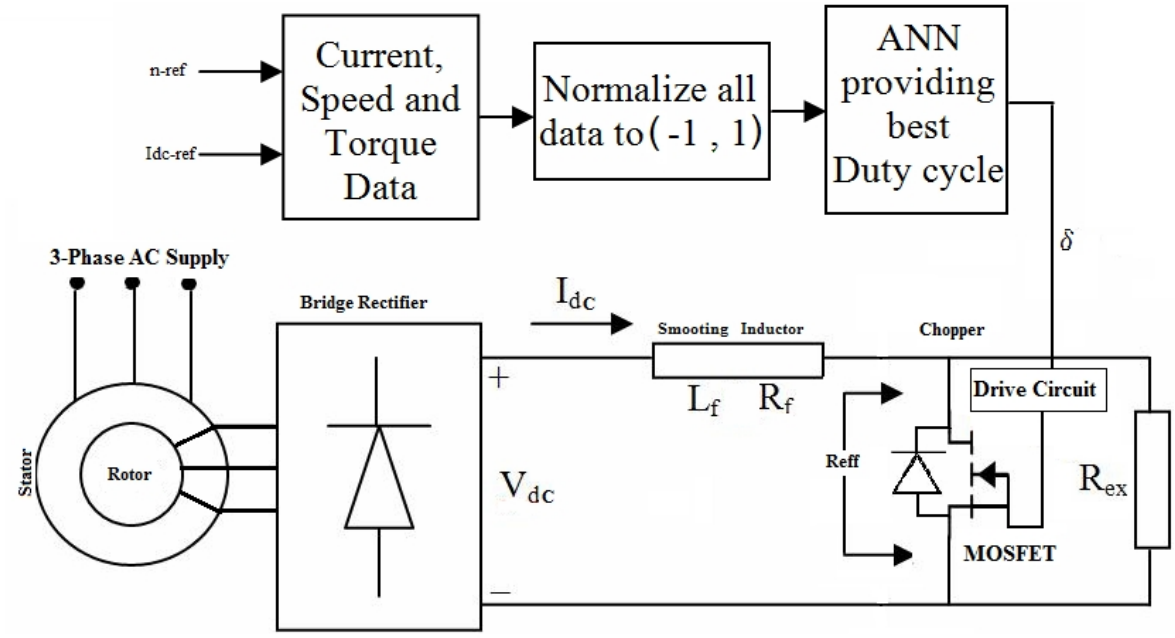

Figure 3. The modified control system diagram

5. Results

Multilayer feed forward networks were chosen to process the prepared input data. In this paper a hundreds of cases for constant speed and constant torque were simulated and appropriated duty cycle value of power MOSFET was obtained. Most of the data was used for training and the rest was applied for testing the networks. ANN simulator has been trained through the 50 epochs. A typical ANN training model was shown in Figure 4.

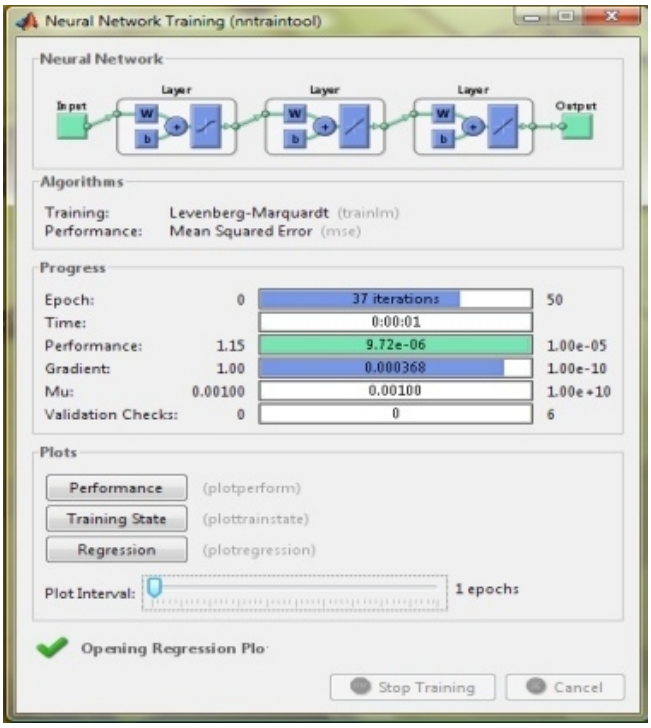

Figure 4. A typical ANN Training Model

Figure 5 shows the variation of the torque developed with rotor rectified current for the actual value and ANN based model. The curves show that the designed ANN model is very near to actual values. Figure 6 shows that the variation of speed and duty cycle for ANN based model and actual values at full load and half load. Figure 7 shows the variation of efficiency versus speed as a function of δ for actual value and ANN base model. Figure 8 shows power factor versus speed at different value of δ for actual value and ANN based model.

The obtained results by testing the ANN were very encouraging for both mode of operation at constant speed and constant torque as shown in Table 1 and Table 2. The MSE was 0.88e-8 at the speed = 1350rpm, 0.518e-8 at the speed = 1050rpm, 2.2857e-8 at the torque = 7Nm and 2.0714e-8 at the torque = 14Nm. Figure 9 show the relation between ANN-based rotor current with speed at different values of duty cycle, which seen that the rotor current increased at increased duty cycle. Also Figure 10 show the relation between ANN-based torque with speed at different values of duty cycle, as seen that the torque also increased at increased duty cycle.

Figures 11 & 12 show the relation between ANN-based rotor current and ANN-based torque with duty cycle respectively. A sample of closed loop ANN-based chopper controller used for constant speed drive and constant torque are shown in Figures 13 and 14. Figure 13 shows the simulation results for constant speed operation. The reference speed is kept constant at 1200rpm, while the load torque is changed suddenly from 7N.m to 14N.m. It is noticed that the motor speed has decreased, but after a second it recovers to its reference value. Figure 14 illustrate the simulation results when the reference speed increased suddenly from 1000rpm to 1200rpm with constant load torque of 7N.m. It is clear that increasing the reference speed increases the chopper duty cycle (δ), while results in decreasing the rotor effective resistance and consequently increasing the motor electric torque during acceleration period. Since the load torque is kept constant an acceleration torque appears which results in acceleration the speed of the motor until it reaches the reference speed.

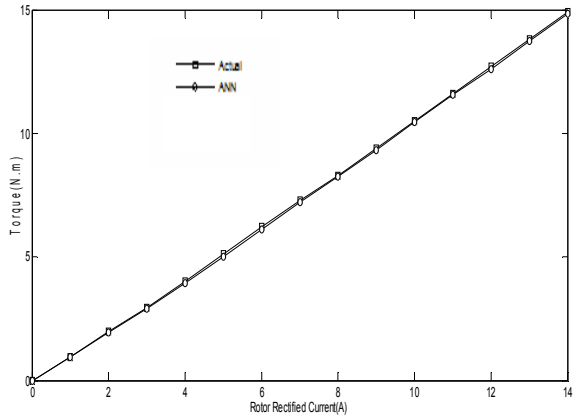

Figure 5. Torque -Idc relationship

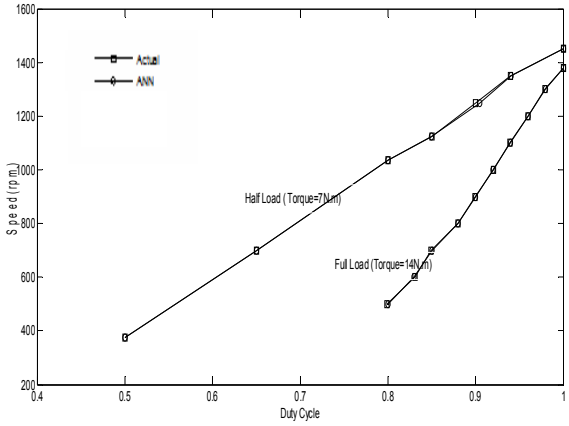

Figure 6. Speed-Duty Cycle relationship at half and full Load Torque

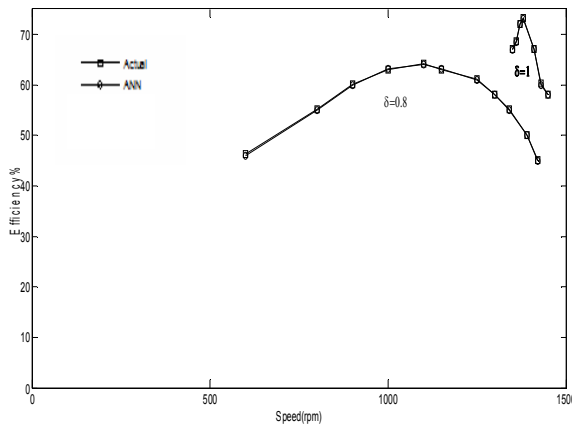

Figure 7. Efficiency-Speed relationship at different δ

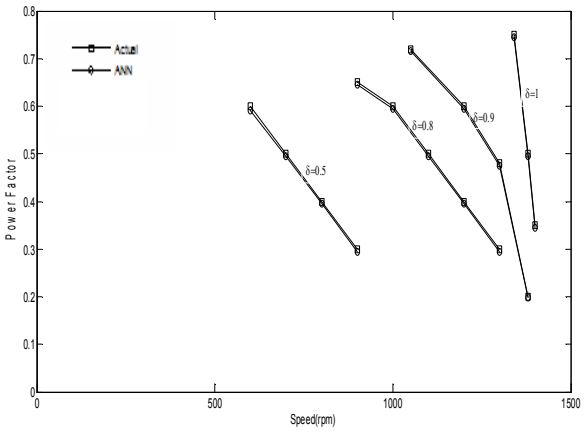

Figure 8. Power factor-speed relationship at different δ

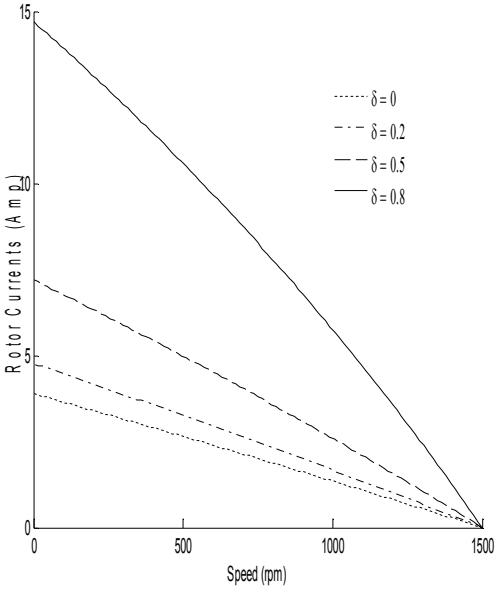

Figure 9. ANN-based rotor speed relationship

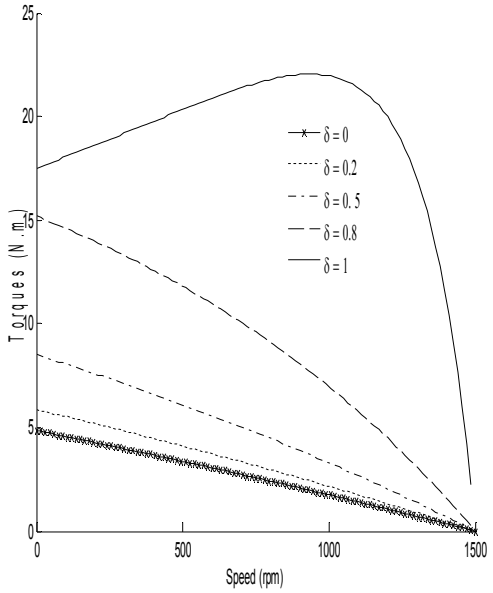

Figure10. ANN-based torque-speed current- relationship

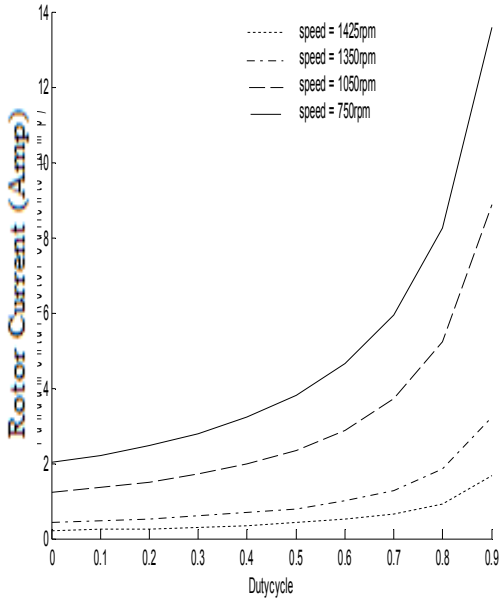

Figure 11. ANN-based current-duty cycle relationship

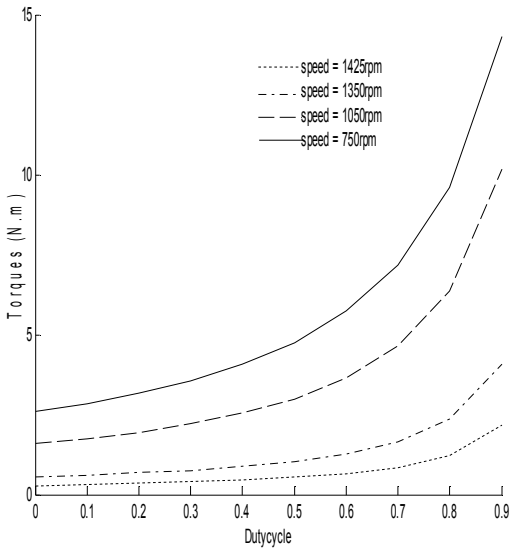

Figure12. ANN-based torque-duty cycle relationship

Table 1. The sample data of ANN-based controller at constant speeds

N=1350rpm				N=1050rpm			
Torque (Nm)	Actual Duty cycle	ANN Duty cycle	Error	Torque (Nm)	Actual Duty cycle	ANN Duty cycle	Error
1	0.56	0.5598	2 E-04	1.5	0.102	0.102	0
2	0.795	0.79504	4E-05	2.5	0.4784	0.4784	0
3	0.8735	0.87346	4E-05	3.5	0.6397	0.6397	0
4	0.9127	0.9126	1E-04	4.5	0.7293	0.7293	0
5	0.9362	0.9361	1E-04	5.5	0.7864	0.7863	1E-04
6	0.9519	0.9518	1E-04	6.5	0.8259	0.82585	5E-05
7	0.9631	0.963	1E-04	7.5	0.8548	0.8548	0
8	0.9715	0.9714	1E-04	8.5	0.877	0.8769	1E-04
9	0.978	0.978	0	9.5	0.8944	0.8944	0
10	0.9832	0.9832	0	10.5	0.9086	0.9085	1E-04
11	0.9875	0.9875	0	11.5	0.9203	0.9202	1E-04
12	0.9911	0.991	1E-04	12.5	0.9301	0.93	1E-04
13	0.9941	0.994	1E-04	13.5	0.9385	0.9384	1E-04
14	0.9967	0.9966	1E-04	14.5	0.9457	0.9456	1E-04

Table 2. The sample data of ANN-based at constant torques.

Torque = 7 N.m				Torque = 14 N.m			
Speed (rpm)	Actual Duty cycle	ANN Duty cycle	Error	Speed (rpm)	Actual Duty cycle	ANN Duty cycle	Error
1440	0.9996	0.9991	5E-04	1365	0.9994	0.9992	2E-04
1380	0.9753	0.9752	1E-04	1305	0.9885	0.9883	2E-04
1320	0.9509	0.9509	0	1245	0.9776	0.9775	1E-04
1260	0.9266	0.9265	1E-04	1185	0.9667	0.9666	1E-04
1200	0.9022	0.9022	0	1125	0.9558	0.9556	2E-04
1140	0.8779	0.8778	1E-04	1065	0.9449	0.9447	2E-04
1080	0.8535	0.8535	0	1005	0.934	0.934	0
1020	0.8292	0.8291	0.0001	945	0.9231	0.923	1E-04
960	0.8049	0.8048	1E-04	885	0.9122	0.912	2E-04
900	0.7805	0.7805	0	825	0.9013	0.9013	0
840	0.7562	0.7561	1E-04	765	0.8904	0.8903	1E-04
780	0.7318	0.7318	0	705	0.8795	0.8795	0
720	0.7075	0.7074	1E-04	645	0.8686	0.8685	1E-04
660	0.6831	0.6831	0	585	0.8577	0.8575	2E-04

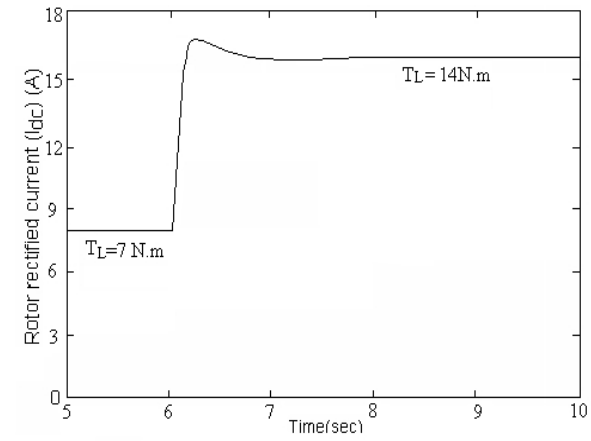

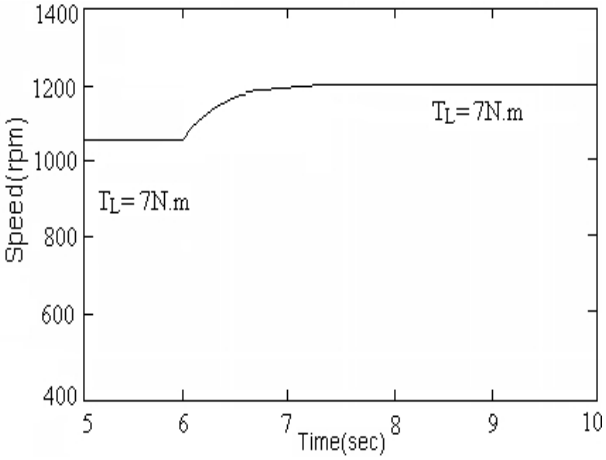

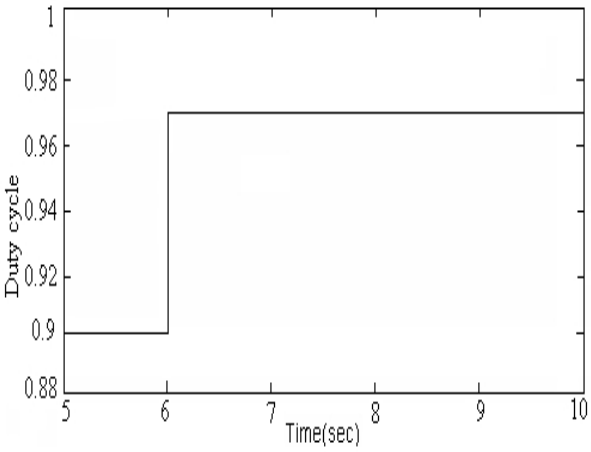

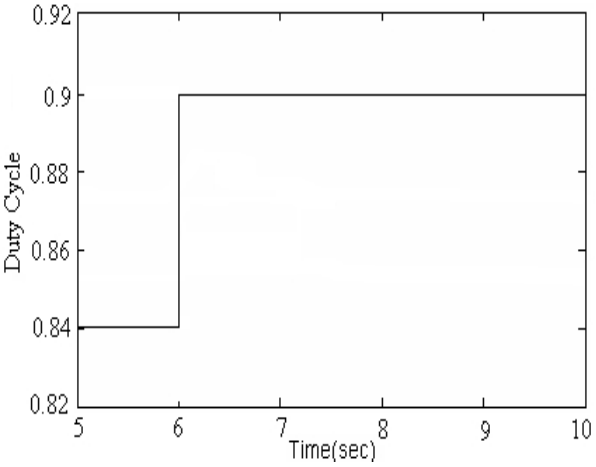

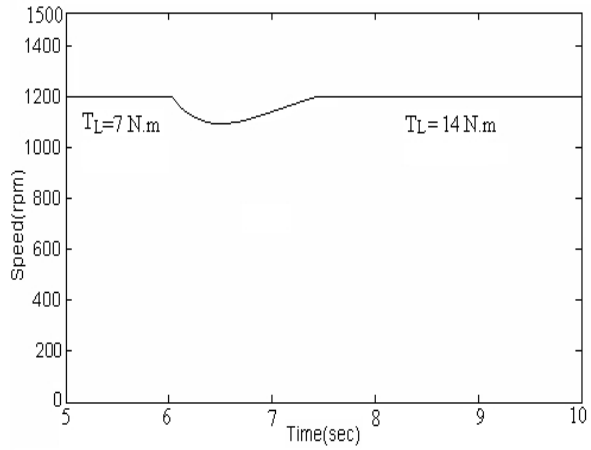

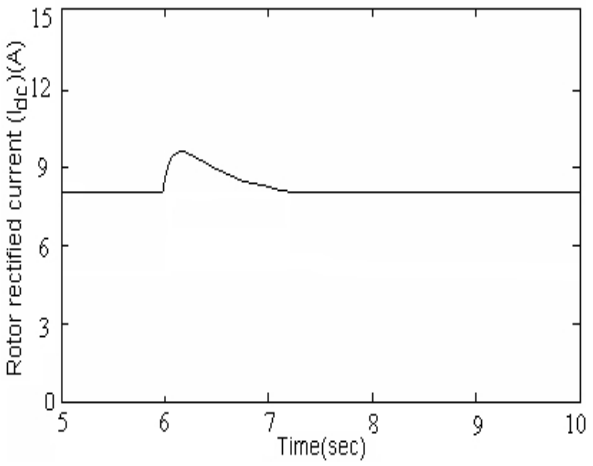

Figure 13. The simulation results of ANN estimator for constant speed drive.

Figure 14. The simulation results of -based ANN- based estimator for constant current drive

Figure 15 and Figure 16 show harmonic currents and harmonic torques with harmonic orders respectively for 0.5 and 0.8 duty cycle and for previous cases of speeds. Figure 17 and Figure 18 show harmonic currents and harmonic torques respectively with the duty cycle for speeds 1425rpm and 750rpm. It is shown that with increasing the duty cycle beyond 0.9 the rotor harmonic current increase rapidly.

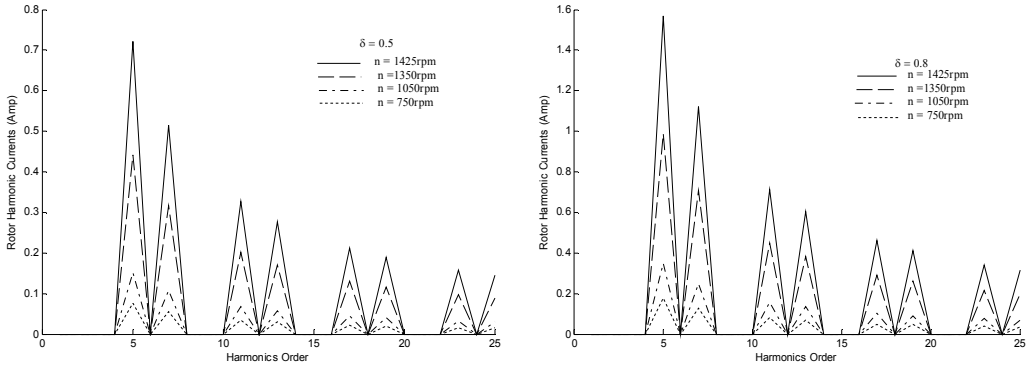

(a) ***(b)***

Figure 15. (a) The relationship of ANN-based harmonic currents with harmonic order at duty cycle 0.5, (b) The relationship of ANN-based harmonic currents with harmonic order at duty cycle 0.8

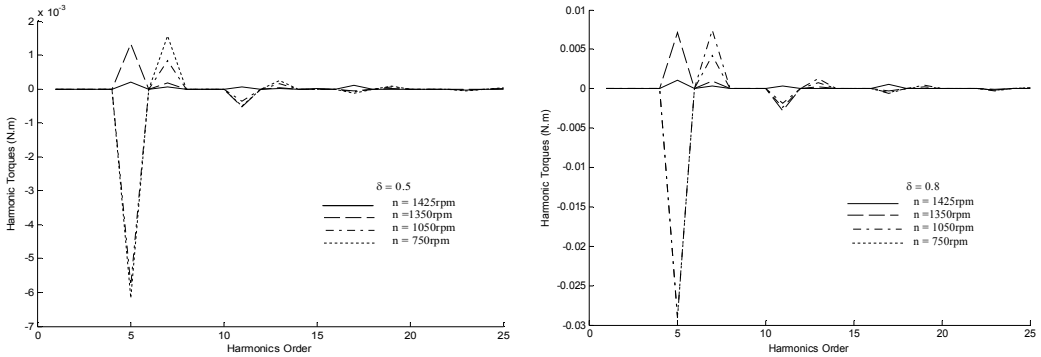

(a) ***(b)***

Figure 16. (a) The relationship of ANN-based harmonic torques with harmonic order at duty cycle 0.5, (b) The relationship of ANN-based harmonic torques with harmonic order at duty cycle 0.8

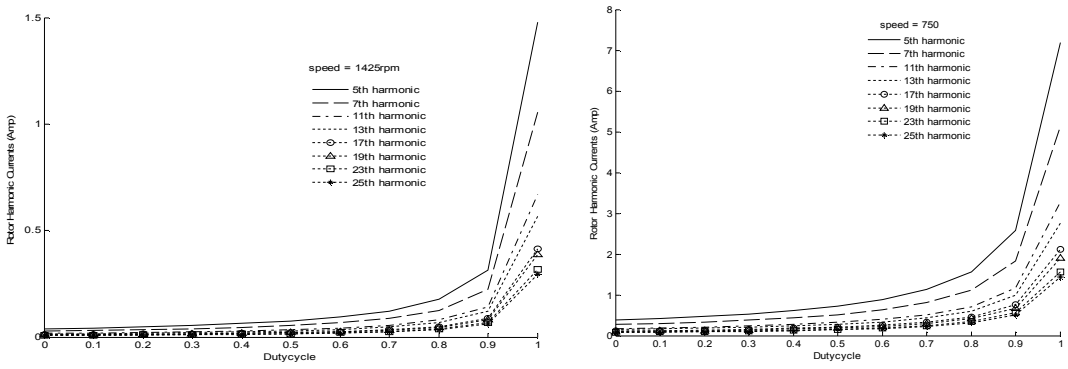

(a) ***(b)***

Figure 17. (a) ANN-based relation of harmonic currents with duty cycle at speed 1425rpm , (b) ANN-based relation of harmonic currents with duty cycle at speed 750rpm

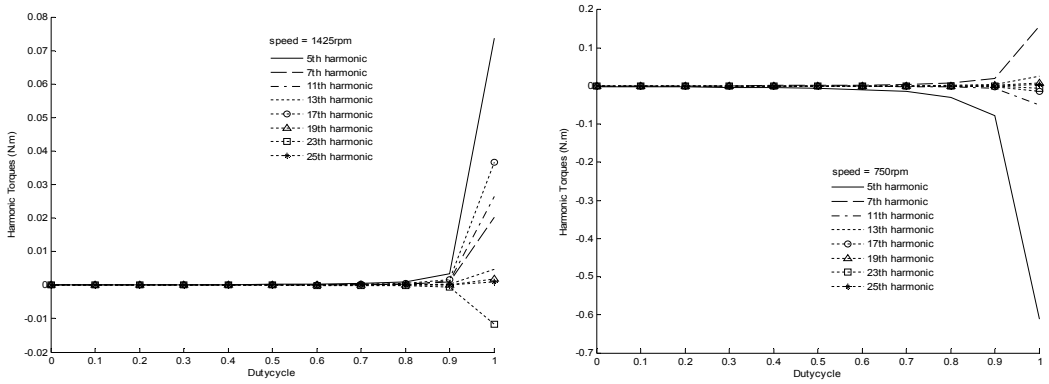

Figure 18. (a) ANN-based relation of harmonic torques with duty cycle at speed 1425rpm, (b) ANN-based relation of harmonic torques with duty cycle at speed 750rpm

6. Conclusion

A small three-phase induction motor is selected for this study and a novel method of adjusting the duty cycle of a chopper-controlled slip ring induction motor has been introduced. The method depends on training a multi-layer ANN model on a set of data generated by a MATLAB simulation program.

The generated data are the motor speed, load torque at different operating conditions as an input and their corresponding chopper duty cycle as an output of the ANN model. The ANN model was trained successfully and the results of comparison between the actual data and the ANN calculated data were satisfactory. Simulation studies are performed and module's performance with different system conditions is investigated.

It was found that ANN application is very accurate and useful for speed control of WRIM. Table 1 and 2 shows that ANN is very quick and reliable to find appropriate duty cycle for chopper resistance WRIM which are concerning to control of speed. According to Table 1 and 2, it is noticed that there is a very good fitting between both ANN and actual results, by which the mean square errors for all testing data for all networks were 0.0008, which proves that the designed ANN model is very precise. Therefore, the neural network has the best capability in WRIM speed control drives.

Current and torque harmonics are also analyzed, which produced by transformation action in the rectifier bridge and chopper circuit in the rotor circuit of the induction motor. The results show the amplitude of the harmonic level depends on the speed of the motor and duty cycle.

7. References

1. P.C. Sen, "Electric Motor Drives and Control – Past, Present and Future", IEEE Trans. on Industrial Electronics, Vol. 37 (6), pp. 562-575, 1990.

2. N. K. Mohantly, R. Muthu, M. S. Kumaran, "A Survey on controlled AC Electrical Drives", Int. J. Elect. Power Eng., Vol. 3, No. 3, pp. 175-183, 2009.

3. M. Ramamorty, M. Arunchalam, "Dynamic performance of a closed loop induction motor speed control system with phase-controlled SCRs in the rotor", *IEEE Trans. on IA.,* Vol. 15, No. 5, pp. 489-493, 1979.

4. P.C. Sen, K.H.J. Ma, "Rotor Chopper Control for induction motor drives: TRC strategy", *IEEE Trans. On IA.*, Vol. 11, No.1, pp. 43-49, Sep/Oct. 1975.

5. S. Joshi, G. Dubey, S. Pillai, "Extension of control range of pulse resistance controlled wound rotor induction motor", *IE(I) Journal-El*, Vol. 61, pp 126-131, Dec. 1980.

6. M.Y. Abdelfattah, A.R. Abdelaziz, "Performance study of chopper-controlled induction motor", *Electric Machine and Power System Journal*. Vol. 19, No. 1, pp. 81-102, Jan. 1991.

7. J.R.Pgupta, Bhim Singh and B.P. Singh, " A closed loop rotor resistance control method for improved DC dynamic braking of WRIM" , IEEE Tran. on IA, Vol.21, No.1, 1985.

8. Chin S Moo, Chung C. Wei, Ching L. Hneg and Chao S. Chen," Starting control of WRIMs by using chopper controlled ressitance in rotor circuit", IEEE confernence of IA society annual conference meeting, 1989, Vol.2, pp 2295-2300.

9. R.M.Hamoud, A.I.Alolab, M.N.badr and m.A. abdalhalim," A comparative study on the starting methods of 3-phase WRIM" IEEE tran. on energy conversion, Vol 14, No.4, 1999.

10. Bimal K. bose, " Artificial neural network applications in power electronics", IECON, the annual conference of the IEEE industrial electronics society . pp 1631-1638.

11. M.Y. Abdelfattah, M. M. Ahmed, "An Artificial Neural Network-Based Chopper-Controlled Slip-Ring Induction Motor", *IEEE* MELECON 2002, Cairo, Egypt, May 2002.

12. N.S.Wani and M. Ramamorty," Chopper controlled slip ring induction motor" IEEE transaction on IECI, Vol.24, No.2, 1977.

13. G. K. Dubay," Power Semiconductor Controlled Drives" 1st edition, Prentice Hall, 1989.

14. P. Pillay Synopsis, E. J. Odendal, R.G. Harley, "Torque and speed harmonic analysis of a PWM CSI-fed induction motor drive", The Transactions of SA Institute of Electrical Engineers, pp.50-59, December 1984.

15. A. K. Mishra, Prof A. K. Wahi, "Performance Analysis and Simulation of Inverter-fed Slip-power Recovery Drive" IE (I) Journal. EL, Vol 85, pp.89-95, September 2004.

16. B. K. Bose, "Modern Power Electronics and Drives", 2nd edition Pearson Education , Asia. 2003.

17. M. Y. Chow, "Methodologies of using neural network and fuzzy logic technologies for motor incipient fault detection" , World Scientific Publishing Co. Pte. Ltd, Singapore, 1997.

18. Y. Birbir, H. S. Nogay Y. Ozel, "Neural Network Solution to Low Order Odd Current Harmonics in Short Chorded Induction Motor" , International Journal of System Applications Engineering and Development, Issue 1, Volume 2, 2008.

19. M.T. Hagan, M. Menhaj, "Training Feed Forward Networks with the Marquardt Algorithm", IEEE. Transaction on Neural Networks, 5(6), pp.989-993, 1999.